

Pre-drilling Effect on Thermal Friction Drilling of Cast Aluminum Alloy Using Thermo-mechanical Finite Element Analysis

Sara Ahmed El-Bahloul

Production & Mechanical Design Engineering Department, Faculty of Engineering, Mansoura University, Mansoura, 35511, Egypt

Received August 18 2020; Revised August 24 2020; Accepted for publication August 24 2020.

Corresponding author: S.A. El-Bahloul (sara_elbahloul@mans.edu.eg)

© 2020 Published by Shahid Chamran University of Ahvaz

Abstract. Thermal friction drilling is a non-conventional hole making process, which uses a rotating tool to penetrate the workpiece and create a bushing. Friction drilling of brittle cast alloys is likely to result in severe petal forming and radial fracturing. This research investigates the effect of pre-drilling diameter and depth on the produced bushing cracks and petal formations while drilling cast aluminum alloy (A380). A three-dimensional finite element model of high-temperature deformation and large plastic strain is performed by using ABAQUS software. Modeling by using dynamic, temperature-displacement, explicit, as well as the adaptive meshing, element deletion, interior contact, and mass scaling techniques, is necessary to enable the convergence of the solution. The finite element analysis results predict that the pre-drilling has a significant effect on the produced bushing shape. The effect of initial deformation decreases with pre-drilling, leading to fewer cracks and petal formations. Hence, the obtained bushing length increases, so providing a more load-bearing surface that leads to a stiffer joint. Additionally, the effect of pre-drilling on the produced temperature is studied, and the results reveal that by increasing the pre-drilling diameter or depth the temperature decreases. Therefore, less workpiece material melting occurs, which leads to less adhering on the tool surface, so fewer cracks and petal formations.

Keywords: Thermal friction drilling; Cast aluminum alloy; Finite element analysis; Pre-drilling; Bushing length; Temperature.

1. Introduction

Thermal friction drilling is a non-conventional drilling process. A rotating tool having a cross-sectional area shown in Fig. 1 (a) approaches to the workpiece surface. The friction occurred between the tool and the workpiece leads to heat generation, which softens the workpiece material and allows tool penetration. Figure 1 (b) illustrates the steps of bushing formation. First, the tool begins initial contact with the workpiece. Next, the tool penetrates the workpiece at the main thrust stage and is encountering a high axial force. The friction force on the contact surface induces heat and softens the workpiece. Then the tool penetrates through the workpiece and creates a hole during the material separating point. This process is used especially for joining thin-walled metal components, as the obtained bushing provides a more load-bearing surface of high strength. Friction drilling is widely used in bearings mounting, heat exchangers, and bicycle frames [1].

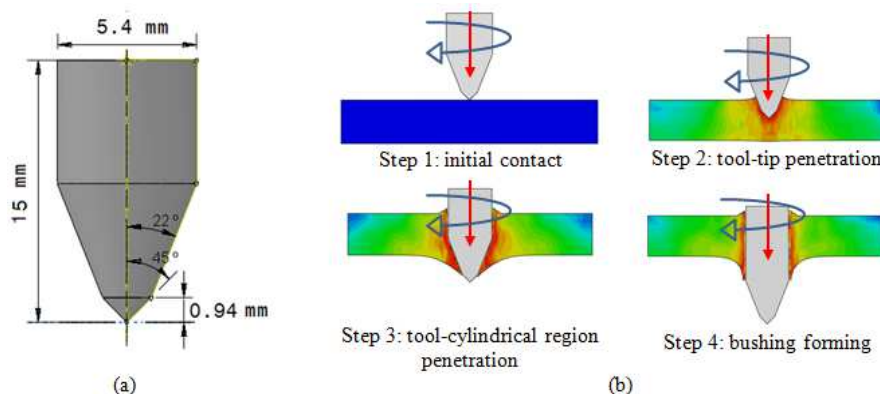


Fig. 1. (a) Friction drilling tool cross-sectional area, (b) Friction drilling steps



Table 1. Tool and workpiece material properties

Material properties	Tool (WC)	Workpiece (A380)	Johnson-Cook parameters
Density (kg/m ³)	15630	2710	A = 324 MPa
Young modulus (GPa)	550	70	B = 159 MPa
Pisson's ratio	0.234	0.33	n = 0.28
Specific heat (J/kg ^o K)	250	870	m = 1.43
Thermal conductivity (W/m ^o K)	84	96.2	Melting temperature = 557 ^o C

Cast aluminum alloy (A380) is one of the most common alloys that is used for a wide variety of important applications. Some of these applications are related to metal joining especially in the automotive industry. [2] It is expected to produce bushing with significant petal formation and radial fracture during friction drilling of brittle cast alloys. According to cracking or peeling in the bushing formation, most of the work-material is displaced improperly and does not create a bushing of the required shape or additional thickness to the threading area [3].

Unfortunately, the publications on the subject of friction drilling relating to finite element analysis of cast alloys are limited. Scott F. Miller et al. used friction drilling to make holes in die-cast metals denoted as Al380 and MgAZ91D. Two ideas were proposed; namely, pre-heating the workpiece and high-speed friction drilling. The results concluded that less severe cracking and petal formation were observed on bushings formed at elevated workpiece temperature. Unfortunately, the bushing shape did not affect by the high spindle speed [3]. Scott F. Miller and Albert J. Shih investigated a three-dimensional finite element modeling for friction drilling of aluminum 6061-T6 using ABAQUS software. The results showed that further improvements are required during the modeling of the process for more accurate simulation [4]. Cebeli Özek and Zülküf Demir investigated the effect of pre-drilling diameter and depth on the bushing shape and the frictional heat in friction drilling of A7075-T651 brittle aluminum alloy. The resultant initial deformation was reduced, leading to bushing formation with fewer cracks and petal formation [5], [6]. Mehmet B. Bilgin et al. conducted a finite element analysis using DEFORM-3D software. An analytic model was developed to calculate the torque and axial power. It was concluded that the torque and axial force values were decreased with increasing the spindle speed, while the temperature was increased with increasing spindle speed [7]. R. Kumar and N. Rajesh Jesudoss Hynes applied the finite element method using DEFORM-3D simulation software to study the friction drilling of galvanized steel [8]. Ekrem Oezkaya et al. developed a three-dimensional finite element method simulation model to predict the tool performance during flow drilling of aluminum cast alloy AlSi10Mg. Nevertheless, the pre-heated tool achieved higher bore quality compared to non-pre-heated flow drills, due to the formability improvement of the cast aluminum alloy at high temperatures [9]. Sara A. El-Bahloul investigated a new idea of producing a cylindrical bushing with no noticeable petal forming and radial fracturing predicted to be obtained through friction drilling of cast aluminum alloy (A380). Three materials are used; namely, 316 stainless steel, aluminum alloy Al6060, and red copper alloy, each of which is placed on the top and bottom surfaces of the A380 workpiece, thereby achieving the idea of functionally graded material. The proposed idea achieved good results especially with red copper sandwich [10]. Shayan Dehghan et al. concerned the thermo-mechanical modeling of friction drilling process on difficult-to-machine materials AISI304, Ti-6Al-4 V, and Inconel718. The numerical simulated results revealed that the main reasons of uniform bushing formation quality for Inconel718, and non-uniform bushing formation quality for Ti-6Al-4 V are due to the high work hardening of Inconel718 and low thermal conductivity of Ti-6Al-4 V [11].

The aim of this work is to study the effect of pre-drilling diameter and depth on the produced bushing while drilling cast aluminum alloy (A380) to reduce the severe petal forming and radial fracturing that is likely to result. This investigation is performed using a three-dimensional finite element model of high-temperature deformation and large plastic strain. The thermo-mechanical finite element analysis is performed by using ABAQUS software.

2. Thermo-Mechanical Finite Element Analysis

Finite element analysis is important to various industries especially those that need to predict the failure of a structure, object, or material. It allows designers to understand all of the theoretical issues without the need for performing difficult experimental work, which in turn reduces the net cost.

The deformation of the workpiece material is very large during thermal friction drilling, and both the tool and workpiece temperatures are high. Modeling is a critical method for understanding material flow, stresses, strains, and temperatures that are hard to experimentally measure during friction drilling. A thermo-mechanical finite element simulation is conducted to determine the attained bushing shape and temperature during the thermal friction drilling process. This simulation is performed using ABAQUS finite element based software.

2.1 Modeled Tool and Workpiece

The modeled thermal friction drilling tool consists of three regions as shown in Fig. 1(a). The first region can be called the center region and it is considered as the tool tip. The cone-shape center angle (α) has an angle equal to 90°. The height of this region is equal to 0.94 mm. This cone angle plays an important role during friction drilling. It causes the blunting effect, which can generate more force and, therefore, heat at the start of the drilling. It looks like the web in a twist drill, which prevents the tool from walking at the start of the process. The second region is called the conical region. This region has a sharper angle than the center region. This angle is commonly called friction angle (β), as this region is the source of friction that leads to more heat and allows tool penetration. The friction angle that is used in the modeling is equal to 44°. The final region is the cylindrical one. This region helps to form the shape of the bushing. The diameter of this region (d) is designated as 5.4 mm. The tool material that is used in this study is tungsten carbide (WC). Table 1 shows the used tool material properties based on the offered tools by Flowdrill Company – Netherlands used previously in different experimental works [12].

The workpiece material that is included in this analysis is the A380 cast aluminum alloy. The implemented material properties are based on a manufactured workpiece used previously in experimental work as a plate of dimensions 145×38×5 mm with chemical composition: Cu 3-4%, Mg 0.1%, Fe 1.3% max., Ti 0.35% max., Ni 0.5 Max., Zn 3% max., Mn 0.50 %, Si 7.5-9.5%. The workpiece manufacturing processes were performed in the Metallurgical Development Research Center – Egypt [10]. Table 1 shows the used workpiece material properties. The material properties that are used for modeling the elastic-plastic behavior of the workpiece material in ABAQUS must be temperature-dependent. Hence, the Johnson-cook model is applied with parameters given in Table 1 [3, 13].

To study the effect of pre-drilling diameter and depth on the produced bushing while drilling A380 cast aluminum alloy, sixteen finite element analysis input settings are modeled in this study, as explained in Table 2. Each of the modeled workpieces is deemed as a disc with an outer diameter (D) and thickness (t) equal to 30 mm and 5 mm respectively. The blank model, which is compared to the other fifteen models, is assumed to be the benchmark. Figure 2 clarifies the diameter and depth of the pre-drilling holes.



Table 2. Thermo-mechanical finite element models

Experiment number	Pre-drilling depth (mm)	Pre-drilling diameter (mm)	Drilling conditions	Bushing length (mm)	Peak temperature (°C)
1	0	0		5.32	709.4
2	1			5.67	679.8
3	2		Tool material: WC	6.43	640.3
4	3	0.94	d = 5.4 mm	6.21	586.2
5	4		β = 44°	6.03	525
6	5		α = 90°	9.29	487
7	1		Rotational speed = 4000 rpm	6.67	567.6
8	2		Feed rate = 160 mm/min	7.24	528.3
9	3	1.88		7.07	480.8
10	4			6.9	434
11	5			8.93	397.7
12	1		Workpiece material: A380	8	482.1
13	2		t = 5 mm	7.93	459.7
14	3	3.7	D = 30 mm	7.68	420.1
15	4			7.59	363.7
16	5			7.5	332.2

2.2 Thermo-Mechanical Model Governing Equation

During the thermal friction drilling process, the friction and the plastic deformation leads to heat generation, which elevates the workpiece temperature. Equations (1) and (2) illustrate the governing equation for the thermal model [12].

$$\rho c \frac{\partial T}{\partial t} = k \left(\frac{\partial^2 T}{\partial x^2} + \frac{\partial^2 T}{\partial y^2} + \frac{\partial^2 T}{\partial z^2} \right) + G \quad (1)$$

$$G = 2\pi R N \mu F_n + \eta \sigma \varepsilon^{pl} \quad (2)$$

where ρ is the density, c is the specific heat, k is the heat conductivity, T is the temperature, t is the time, G is the heat generation rate, x , y , and z are the coordinates, η is the inelastic heat fraction, σ is the effective stress, and ε^{pl} is the plastic strain rate. The heat generation rate G consists of the heating rate due to the friction between the rotating tool and the stationary workpiece, and the heating rate caused by the plastic deformation inside the workpiece.

2.3 Thermo-Mechanical Model Techniques

Four finite element analysis techniques are applied during the modeling of the thermal friction drilling process; namely, adaptive meshing, element deletion, internal contact and mass scaling.

In certain nonlinear simulations, the material undergoes very large deformations in the structure or phase. Such deformations distort the finite element mesh, often to the extent that, the mesh is unable to produce correct data, or the study terminates for computational reasons. In these simulations, adaptive meshing tools are used to mitigate the distortion in the mesh periodically. Hence, the adaptive meshing technique retains a good quality mesh in the solution by adjusting the mesh to recover extremely distorted elements aspect ratio.

The element deletion technique allows tool penetration into the workpiece by elements separation. Elements deactivation occurs with excessively large plastic strain. In this analysis, the value of the equivalent plastic strain on which the deletion of the element is dependent is equal to 2.

Mass scaling is implemented to improve the finite element analysis computational efficiency with keeping the accuracy high. Throughout this analysis, mass scaling is done every 10 increments to achieve a consistent 0.0001s step time increment.

For the proposed models, contact may occur both on the outside and inside of regions that may be eroded due to the failure of workpiece material. The general contact that is supported in ABAQUS is not appropriate or not sufficient for the proposed model. The general contact domain can be modified by including and/or excluding predefined contact surfaces by performing the following steps:

1. Creating the model with an exterior surface and plate element set.
2. Modifying the resulting input file by adding the following code before the end of the assembly:

```
SURFACE, type=ELEMENT, NAME=ERODE
```

```
, PLATE, INTERIOR
```

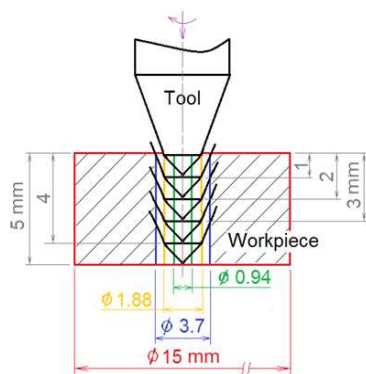


Fig. 2. The pre-drilling holes diameter and depth illustration

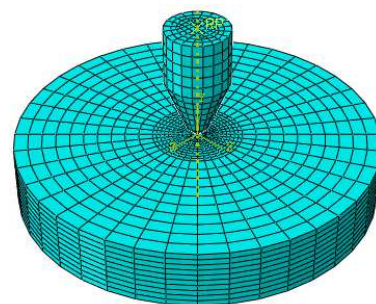


Fig. 3. The meshed tool and workpiece



This code defines an element-based surface that includes the exterior and interior faces of the eroding plate. Modification of the contact inclusion code from 'ALL EXTERIOR' to 'TOOL, ERODE' is performed, where the PLATE is an element set containing all the plate continuum elements in the workpiece, and the TOOL is the external surfaces of the tool.

2.4 Meshing and Boundary Conditions

Figure 3 shows the complete meshed model assembly for the blank workpiece and the tool. The outer surface of the workpiece is restricted in all directions. The top and the bottom surfaces of the workpiece are under free convection with a convection coefficient equal to 20 W/m²K and an ambient air temperature of 22°C. The modeled tool is rotated at 4000 rpm. The tool penetration into the workpiece is modeled with a feed rate equal to 160 mm/min. A rigid body constraint is applied to the rotating tool in order to prevent its deformation. A coaxially between the rotating tool and the fixed workpiece is accomplished.

The ABAQUS mesh generator is applied. Eight nodes thermally coupled brick, trilinear displacement and temperature, reduced integration, and hourglass control (C3D8RT) element is used to model the workpiece and the tool. For the modeled tool, the number of elements is 600. For the modeled workpiece in experiment number one, i.e. benchmark experiment, the number of elements is 11000. Certainly, the number of elements for pre-drilling models decreased by increasing the hole depth and/or the hole diameter. Some partitions are accomplished in the workpiece to make the mesh finer near the tool tip as shown in Fig. 2, where the largest material deformation is expected to occur. The size of the element is meaningful to the simulation. If the mesh is too coarse, there will be extreme distortion and loss of too many components, resulting in inadequate bushing shape. On the opposite, if the mesh becomes too fine, processing time dramatically increased without increasing the performance. Hence, choosing the proper element size is an important issue.

Heat partition occurs at the interface between the tool and the workpiece. For frictional heat generation at the tool-workpiece interface, 100 % of the dissipated energy caused by friction is assumed to be converted to heat. A specific heat partition model depending on the tool and workpiece materials heat conductivity ratio specifies the heat partition at the tool-workpiece interface. The ratio of heat partition into the workpiece can be calculated using Equ. (3) [4].

$$r_{wp} = \frac{k_{wp}}{k_{wp} + k_{tool}} \tag{3}$$

where k_{wp} and k_{tool} are the thermal conductivity of workpiece and tool, respectively. At room temperature, k_{wp} of the A380 workpiece is 96.2 W/m²K, while the k_{tool} of the WC tool is 84 W/m²K. Hence, the ratio of heat generated in the tool-workpiece interface transfer to the workpiece is equal to 0.534, i.e., certainly half of the generated frictional heat is transferred to the workpiece.

2.5 Thermo-Mechanical Model Validation

Experimental work is performed for experiment number 1 on a manufactured thermal friction drilling machine [10]. The resultant axial force is measured during friction drilling by a multi-component dynamometer (Kistler-type 9257B; measuring range – 5 to10 kN). Figure 4 shows a comparison between the resultant axial force curve obtained from experimental work and the resultant axial force curve obtained from the analytical simulation at a different coefficient of friction. The results show a similar trend between the experimental work and the analytical simulation at a coefficient of friction equals to 0.1. It is obvious that the axial force finite element analysis profiles are shifted to the left compared to the experimental profile. This is due to the noticeable deflection of the workpiece at the initial contact stage.

3. Results and Discussion

3.1 Effect of Pre-Drilling Depths and Diameters on the Bushing Shape

Figure 5 shows the produced bushing of the blank model, which is assumed to be the benchmark. It is obvious that the produced bushing suffers from significant petal formation and radial fracture. Figure 6 shows the produced bushing of the fifteen experiments illustrated in Table 2. It is clear that pre-drilling has a significant effect on the produced bushing shape. The initial deformation happens when the amount of frictional heat reaches about 1/2 to 2/3 of the workpiece material melting temperature. In the case of pre-drilling, the deformation occurs either when the tool tip starts to contact the workpiece surface at a pre-drilling hole depth of 1, 2, 3, 4, or 5 mm, or when the peripheral diameter of the tool tip is equal to the pre-drilling hole diameter of 0.94, 0.18, and 3.7. The effect of initial deformation decreases with pre-drilling, leading to fewer cracks and petal formations as seen in Fig. 6.

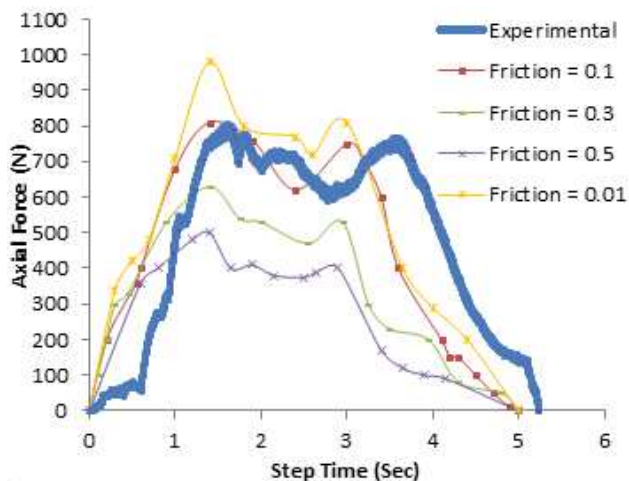


Fig. 4. Thermo-mechanical model validation

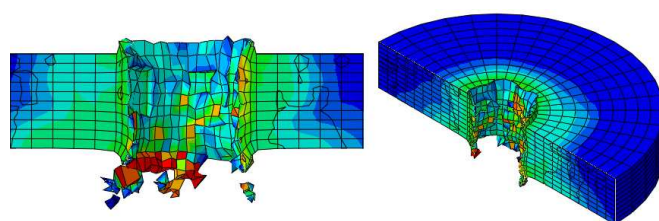


Fig. 5. The produced bushing of experiment number one (benchmark experiment)



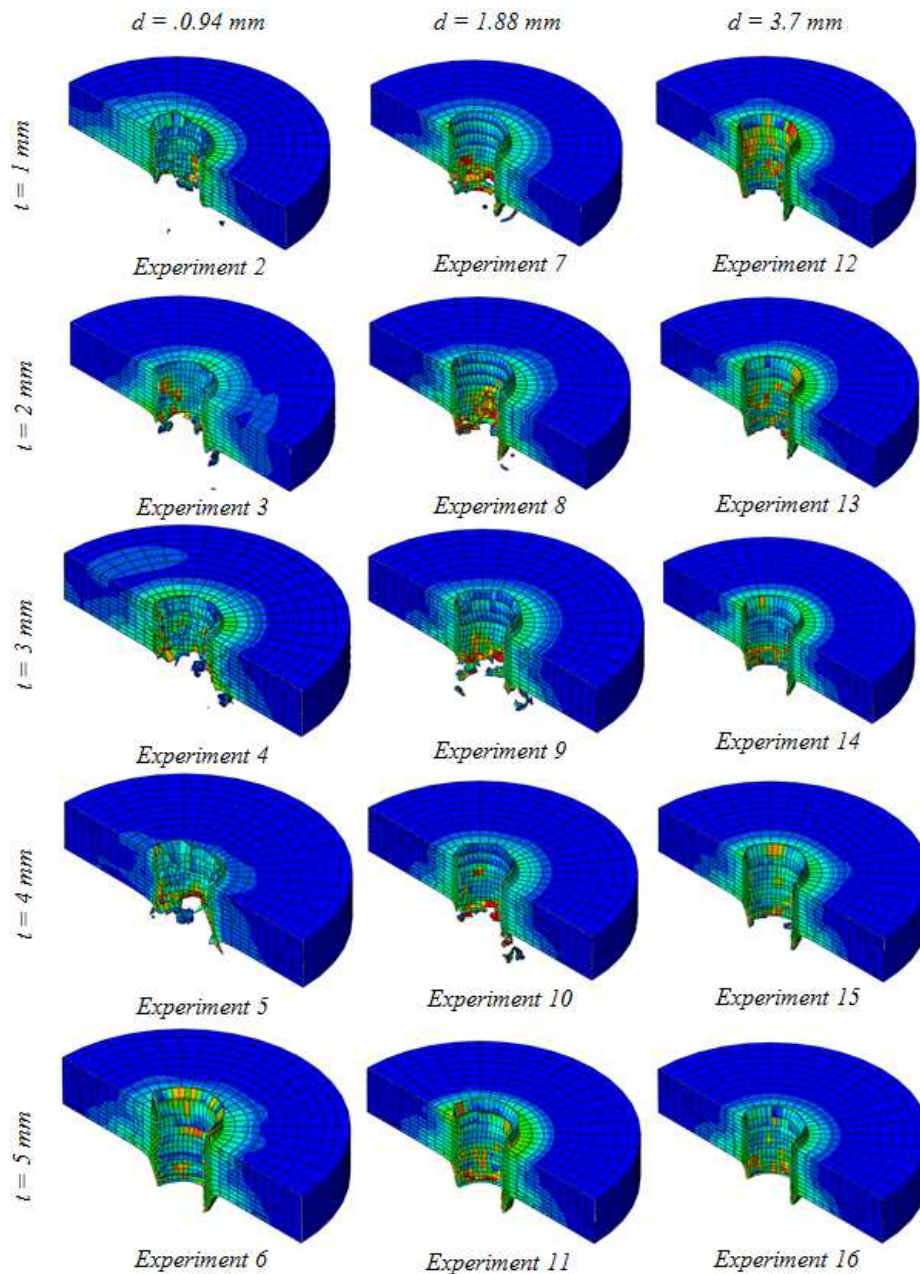


Fig. 6. The produced bushing for experiments number 2 to 16

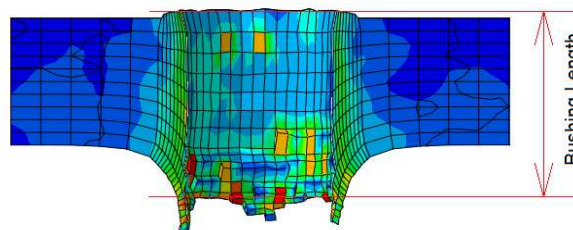


Fig. 7. The bushing length that can be threaded

To determine the effect of pre-drilling on the bushing, the bushing length is measured. Figure 7 illustrates the bushing length, which includes only the length that can be threaded. Figure 8 shows the improvement of the bushing length with pre-drilling at different diameters and depths compared to the benchmark experiment shown in Fig. 5. Fewer cracks and petal formations occur in the case of pre-drilling especially for experiments with larger pre-drilling diameter and depth. Hence, pre-drilling has a positive effect on the obtained bushing length, as it provides a more load-bearing surface that leads to a stiffer joint. Table 2 shows the measured bushing length for the sixteen experiments. Figure 9 (a) illustrates the effect of pre-drilling diameters and depths on the bushing length. The results reveal that the maximum bushing length that can be threaded is obtained with the minimum pre-drilling diameter that equals to 0.94 mm, and a maximum pre-drilling depth equals to 5 mm. Additionally, no petal forming and radial fracturing occur at applying the maximum pre-drilling depth for all the pre-drilling diameters as illustrated in Fig. 8.



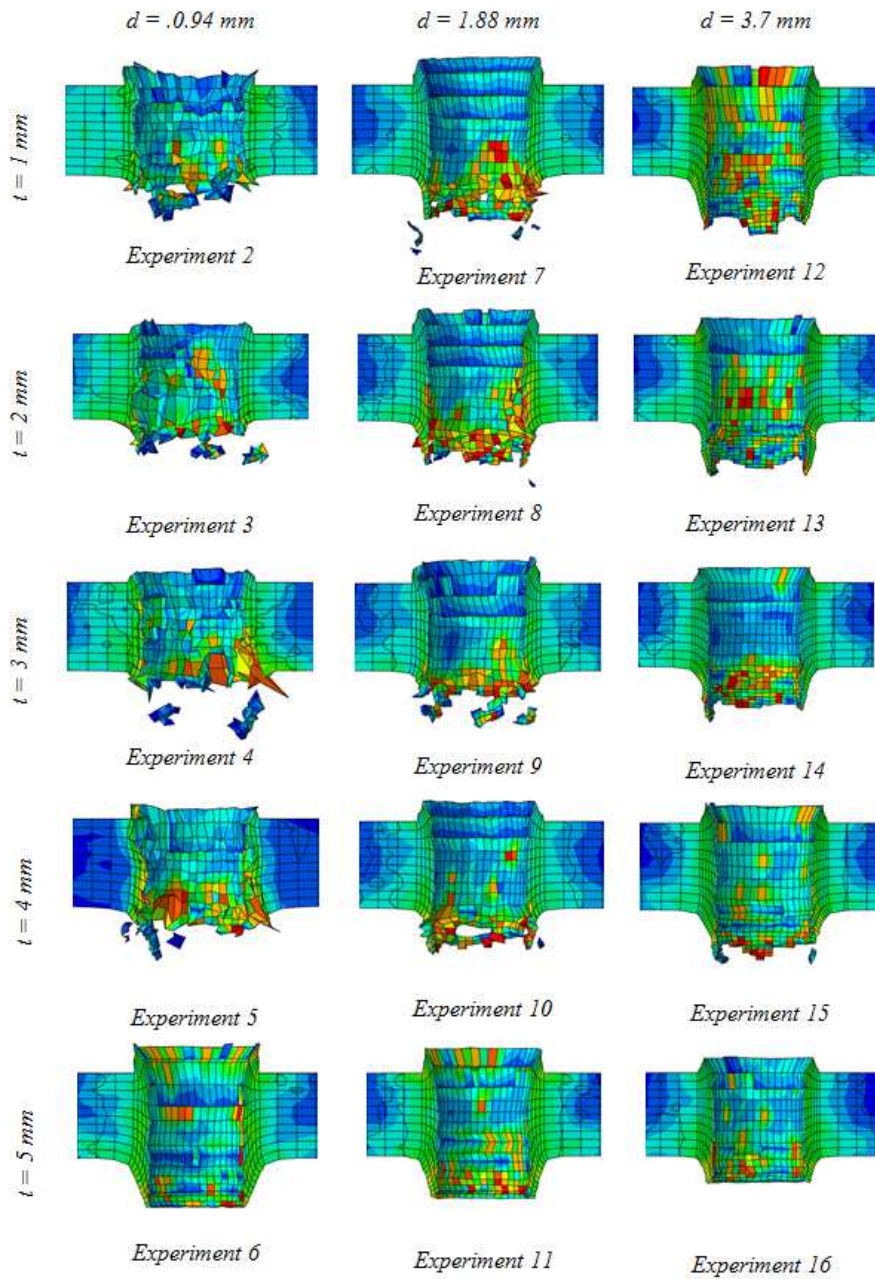


Fig. 8. The improvement of the bushing length with pre-drilling at different diameters and depths

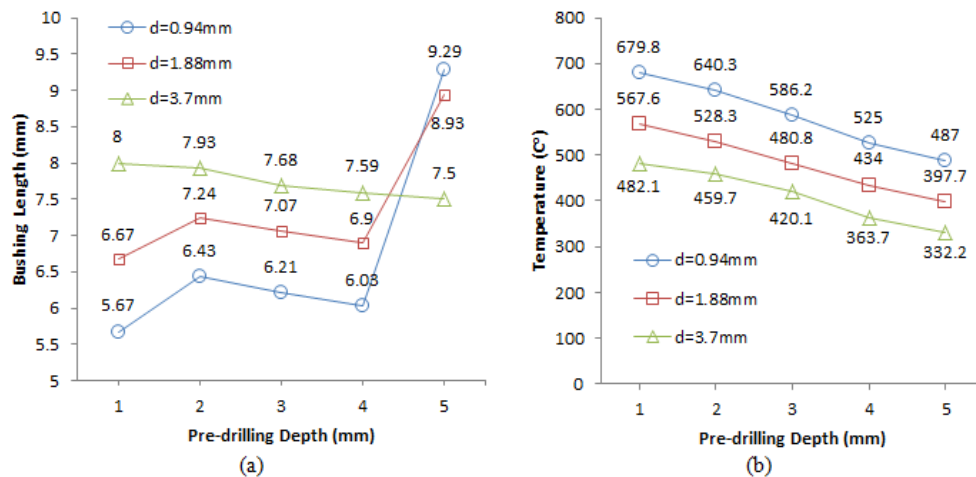


Fig. 9. (a) The effect of pre-drilling diameters and depths on the bushing length, (b) The effect of pre-drilling diameters and depths on the temperature



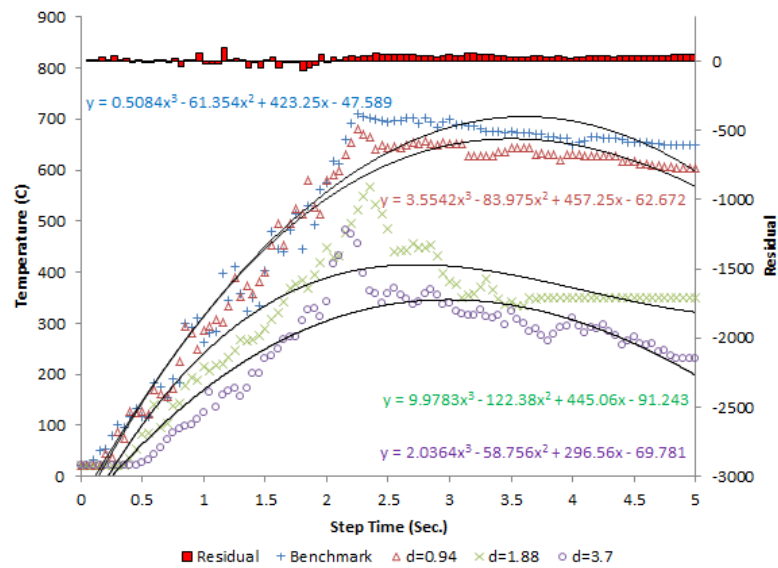


Fig. 10. The obtained temperature trendline at a pre-drilling diameter of 0.94, 1.88, or 3.7 mm and 1 mm depth

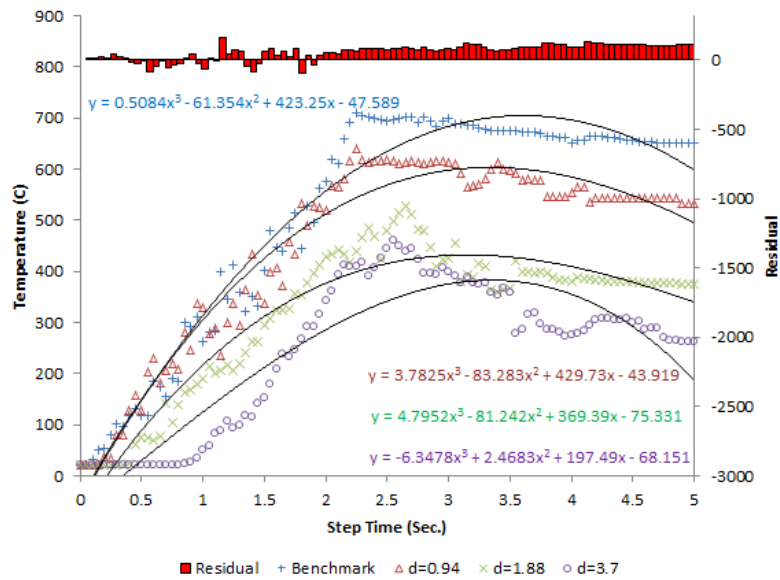


Fig. 11. The obtained temperature trendline at a pre-drilling diameter of 0.94, 1.88, or 3.7 mm and 2 mm depth

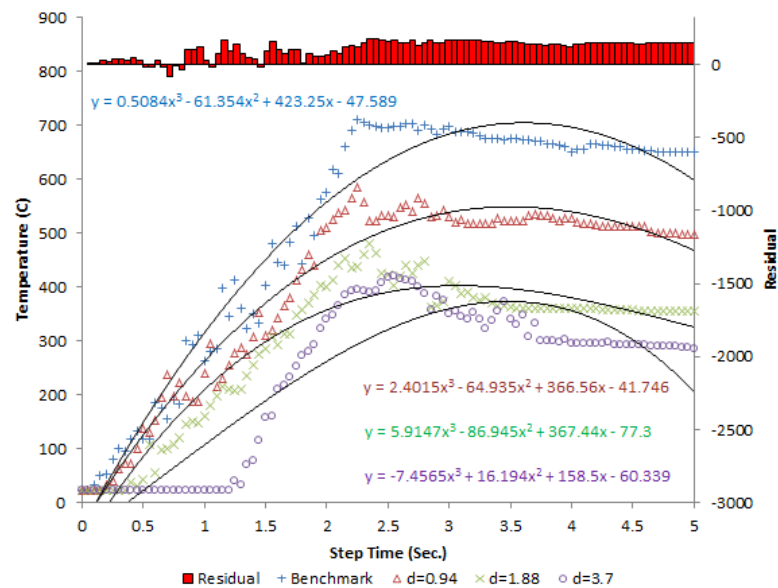


Fig. 12. The obtained temperature trendline at a pre-drilling diameter of 0.94, 1.88, or 3.7 mm and 3 mm depth



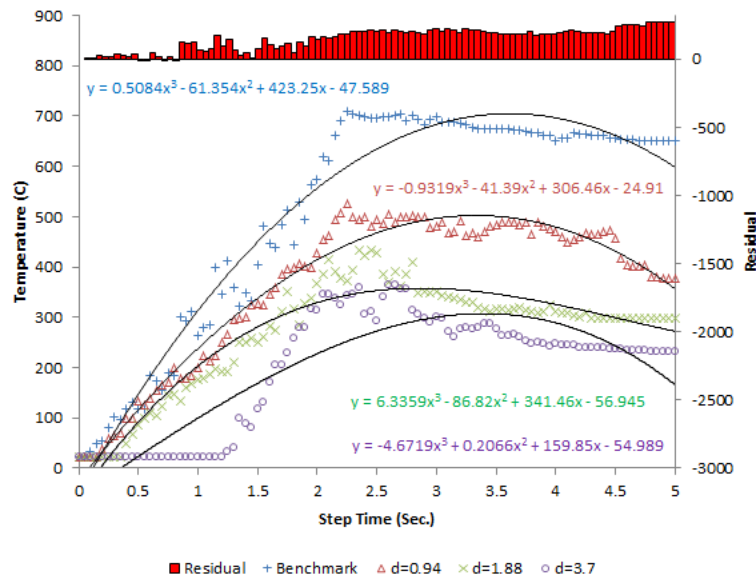


Fig. 13. The obtained temperature trendline at a pre-drilling diameter of 0.94, 1.88, or 3.7 mm and 4 mm depth

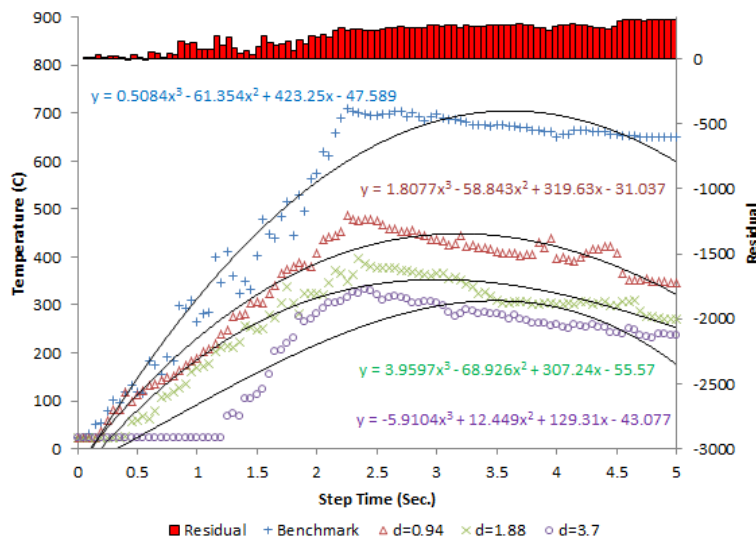


Fig. 14. The obtained temperature trendline at a pre-drilling diameter of 0.94, 1.88, or 3.7 mm and 5 mm depth

3.2 Effect of Pre-Drilling Depths and Diameters on the Temperature

The produced temperature in the bushing that occurs during friction drilling is studied. Figures 10-14 illustrate the obtained temperature trendline curve at the pre-drilling of different diameters and depths. In general, it is clear that the temperature gradually increases until it reaches the peak value when the tool completely penetrates the workpiece thickness. Then the temperature begins to decrease until bushing formation is ended. Table 2 shows the resultant peak temperature for the sixteen experiments. Figure 9 (b) illustrates the effect of pre-drilling diameters and depths on the temperature. It is clear that by increasing the pre-drilling diameter the temperature decreases. The residual values are illustrated in Figs. 10-14 represent the difference between the benchmark temperature and the temperature of the produced bushing at a pre-drilling of 0.94 mm diameter at different depths. From the residual bars illustrated in Fig. 10-14, it is obvious that the maximum residual obtained with a pre-drilling depth of 5 mm. That's mean that by increasing the pre-drilling hole depth, the temperature decreases, as illustrated in Fig. 9 (b).

The trendline equations of the temperature curves for different pre-drilling depths and diameters are given in Figs. 10-14. Each equation can define the relationship between the temperature and the step time. These equations are considered as a third-order polynomial with a higher correlation.

4. Conclusion

This research investigates the effect of pre-drilling diameter and depth on the produced bushing cracks and petal formations while drilling cast aluminum alloy (A380). Throughout thermal friction drilling, the deformation of the workpiece material is very large, and both the tool and workpiece temperatures are high. Modeling is a needed method for knowing the material flow, stresses, strains, and temperatures that are hard to experimentally measure during friction drilling. A three-dimensional thermo-mechanical finite element model of high-temperature deformation and large plastic strain is investigated by using ABAQUS software. Modeling by using dynamic, temperature-displacement, explicit, as well as the adaptive meshing, element deletion, interior contact, and mass scaling techniques, is necessary to enable the convergence of the solution. The finite element analysis results predict that the pre-drilling has a significant effect on the produced bushing shape. The effect of initial deformation decreases with pre-drilling, leading to fewer cracks and petal formations. Hence, the obtained bushing length is increased, so



providing a more load-bearing surface that leads to a stiffer joint. The maximum bushing length that can be threaded is obtained with the medium pre-drilling diameter that equals to 1.88 mm, and a pre-drilling depth equal to 2 mm. Additionally, the effect of pre-drilling on the produced temperature is studied, and the results reveal that by increasing the pre-drilling diameter or depth the temperature decreases. Therefore, less workpiece material melting occurs, which leads to less adhering on the tool surface, so fewer cracks and petal formations. The proposed modeling idea has proven its success and precision since it is powerful for simultaneous simulation of multiple quality features in the thermal friction drilling process.

Acknowledgments

The author would like to acknowledge the Faculty of Engineering – Mansoura University – Egypt for providing the required facilities in performing the experimental work.

Conflict of Interest

The author declared no potential conflicts of interest with respect to the research, authorship, and publication of this article.

Funding

The author received no financial support for the research, authorship, and publication of this article.

Nomenclature

ρ	Material density	T	Temperature
c	Specific heat	t	Time
k	Heat conductivity	G	Heat generation rate
d	Tool cylindrical region diameter	D	disc outer diameter

References

- [1] G. Urbikain, J. M. Perez, L. N. Lopez de Lacalle, and A. Andueza, Combination of friction drilling and form tapping processes on dissimilar materials for making nutless joints, *Proc. Inst. Mech. Eng. Part B J. Eng. Manuf.*, 232(6), 2018, 1007-1020.
- [2] C. A. Muñoz-Ibáñez, M. Alfaro-Ponce, G. Perez-Lechuga, and J. A. Pescador-Rojas, Design and Application of a Quantitative Forecast Model for Determination of the Properties of Aluminum Alloys Used in Die Casting, *Int. J. Met.*, 13(1), 2019, 98-111.
- [3] S. F. Miller, J. Tao, and A. J. Shih, Friction drilling of cast metals, *Int. J. Mach. Tools Manuf.*, 46(12-13), 2006, 1526-1535.
- [4] S. F. Miller and A. J. Shih, Thermo-Mechanical Finite Element Modeling of the Friction Drilling Process, *J. Manuf. Sci. Eng.*, 129(3), 2007, 531.
- [5] Z. Demir and C. Özek, Investigate the effect of pre-drilling in friction drilling of A7075-T651, *Mater. Manuf. Process.*, 29(5), 2014, 593-599.
- [6] Z. Demir, An Experimental Investigation of the Effect of Depth and Diameter of Pre-drilling on Friction Drilling of A7075-T651 Alloy, *J. Sustain. Constr. Mater. Technol.*, 1(2), 2016, 46-56.
- [7] M. B. Bilgin, K. Gök, and A. Gök, Three-dimensional finite element model of friction drilling process in hot forming processes, *Proc. Inst. Mech. Eng. Part E J. Process Mech. Eng.*, 231(3), 2017, 548-554.
- [8] R. Kumar and N. R. J. Hynes, Finite-element simulation and validation of material flow in thermal drilling process, *J. Brazilian Soc. Mech. Sci. Eng.*, 40(3), 2018, 1-10.
- [9] E. Oezkaya, S. Hannich, and D. Biermann, Development of a three-dimensional finite element method simulation model to predict modified flow drilling tool performance, *Int. J. Mater. Form.*, 12(3), 2019, 477-490.
- [10] S. A. El-Bahloul, Friction Drilling of Cast Aluminum Alloy A380 Without Significant Petal Formation and Radial Fracture, *Int. J. Precis. Eng. Manuf.*, 20(1), 2019, 45-52.
- [11] S. Dehghan, E. Souri, and others, A thermo-mechanical finite element simulation model to analyze bushing formation and drilling tool for friction drilling of difficult-to-machine materials, *J. Manuf. Process.*, 57, 2020, 1004-1018.
- [12] S. A. El-Bahloul, H. E. El-Shourbagy, A. M. El-Bahloul, and T. T. El-Midany, Experimental and Thermo-Mechanical Modeling Optimization of Thermal Friction Drilling for AISI 304 Stainless steel, *CIRP J. Manuf. Sci. Technol.*, 20, 2018, 84-92.
- [13] S. Gupta, S. Abotula, and A. Shukla, Determination of johnson-cook parameters for cast aluminum alloys, *J. Eng. Mater. Technol. Trans. ASME*, 136(3), 2014, 034502.

ORCID iD

Sara Ahmed El-Bahloul  <https://orcid.org/0000-0002-4691-4161>



© 2020 by the authors. Licensee SCU, Ahvaz, Iran. This article is an open access article distributed under the terms and conditions of the Creative Commons Attribution-NonCommercial 4.0 International (CC BY-NC 4.0 license) (<http://creativecommons.org/licenses/by-nc/4.0/>).

How to cite this article: El-Bahloul S.A. Pre-drilling Effect on Thermal Friction Drilling of Cast Aluminum Alloy Using Thermo-mechanical Finite Element Analysis, *J. Appl. Comput. Mech.*, 6(SI), 2020, 1371-1379. <https://doi.org/10.22055/JACM.2020.34682.2455>

